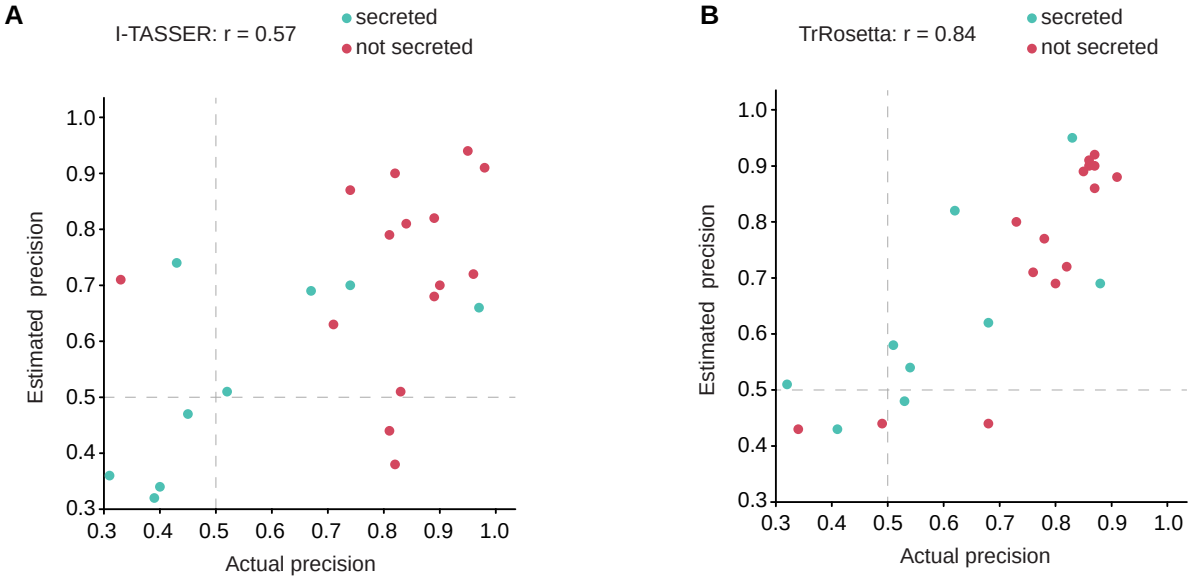

Figure S1. The estimated and actual precision of the structures predicted by I-TASSER and TrRosetta

For the 24 *Maganporthe* proteins with solved structures, the estimated and actual precisions are provided in **A** and **B** for I-TASSER and TrRosetta, respectively. The mean expected TM-score and the average probability of the top L predicted long+medium range contacts (|i-j|>12) represent the estimated precision for I-TASSER and TrRosetta, respectively. These metrics are known to well corelate with the actual precision. The actual precision was obtained by superposing the computational models from I-TASSER or TrRosetta with experimentally determined structures with TM-align. The correlation coefficient (r) between the estimated and actual precision is indicated. The secreted and non-secreted proteins are represented in different colors.

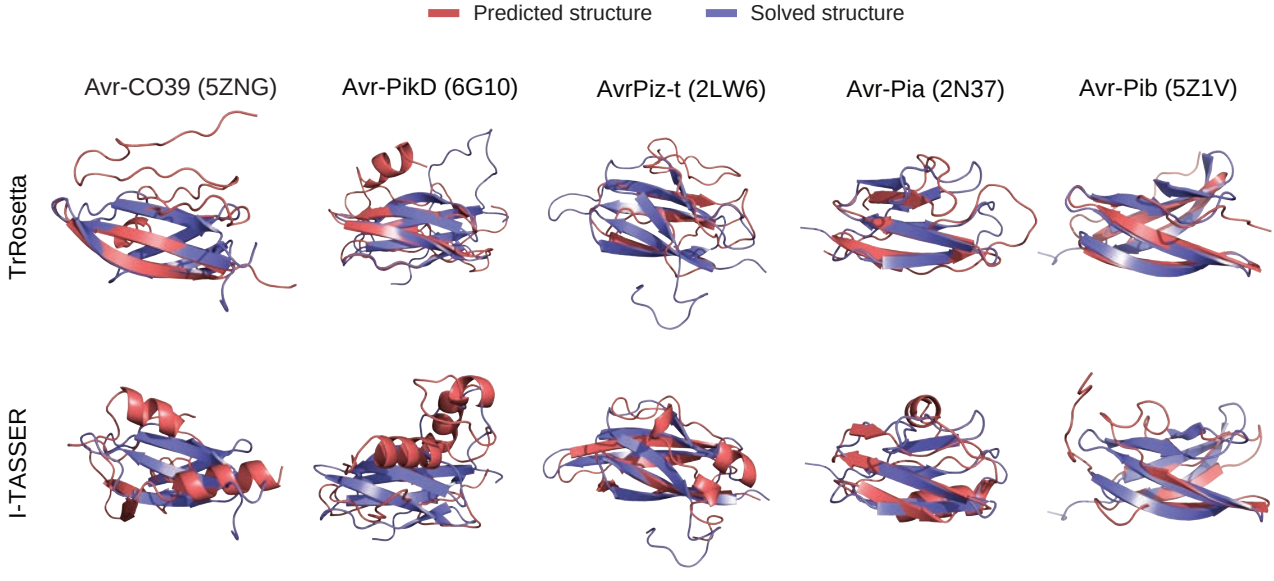

Figure S2. Structural superposition between the predicted and solved structures

The structures of the avirulence effectors predicted by TrRosetta and I-TASSER were superposed with TM-align against their experimentally determined structures. The predicted and solved structures are indicated in red and blue, respectively.

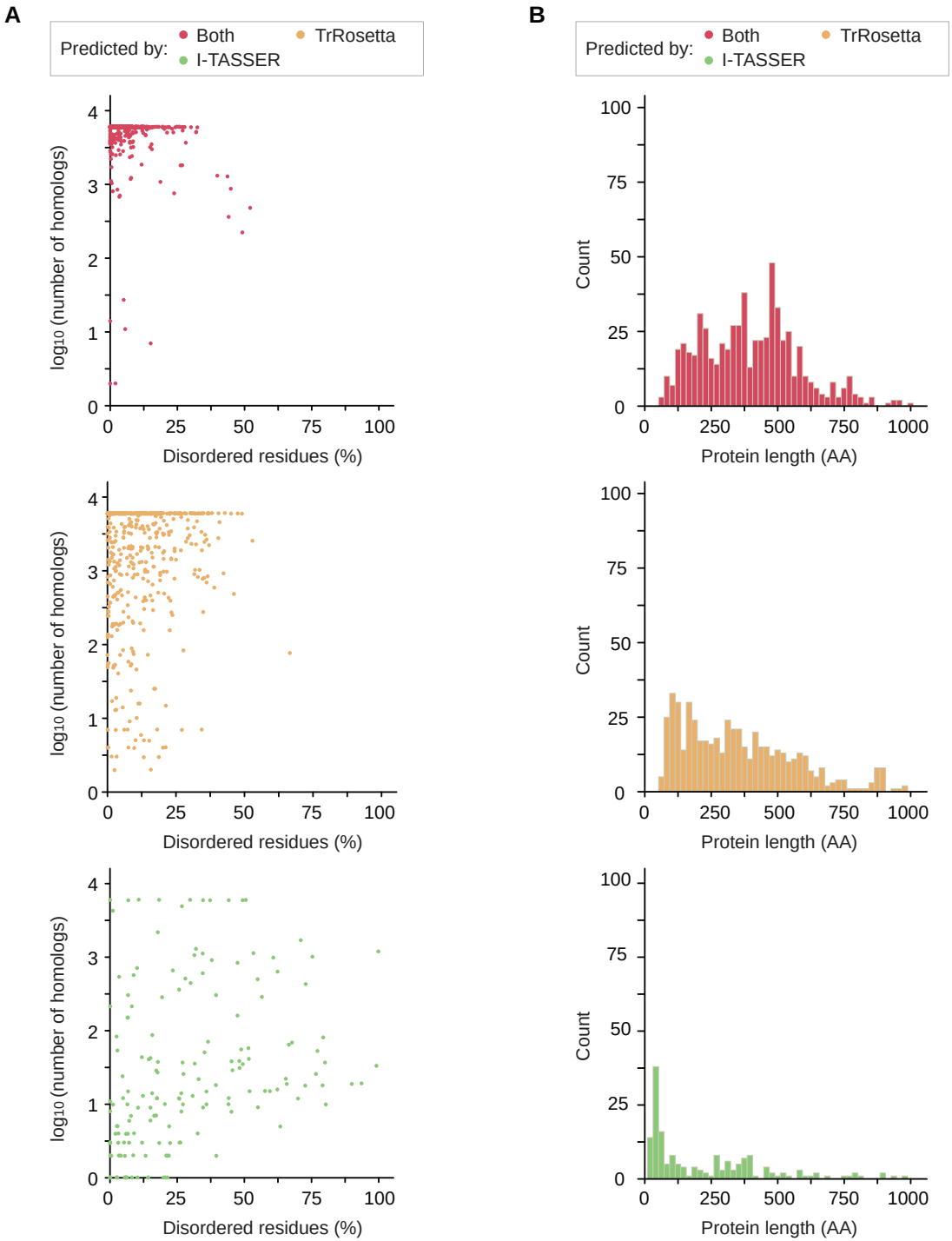

Figure S3. The features of the proteins in the prediction categories

For the four prediction categories in Fig. 2A (prediction by TrRosetta, I-TASSER, both or none), **A,** the proportion of disordered residues and the number of collected homologs and **B,** the length distribution of the mature proteins are provided. The number of homologs is capped at 6,000 and provided on a log scale. The length of the proteins and the proportion of disordered residues were calculated based on the mature proteins.

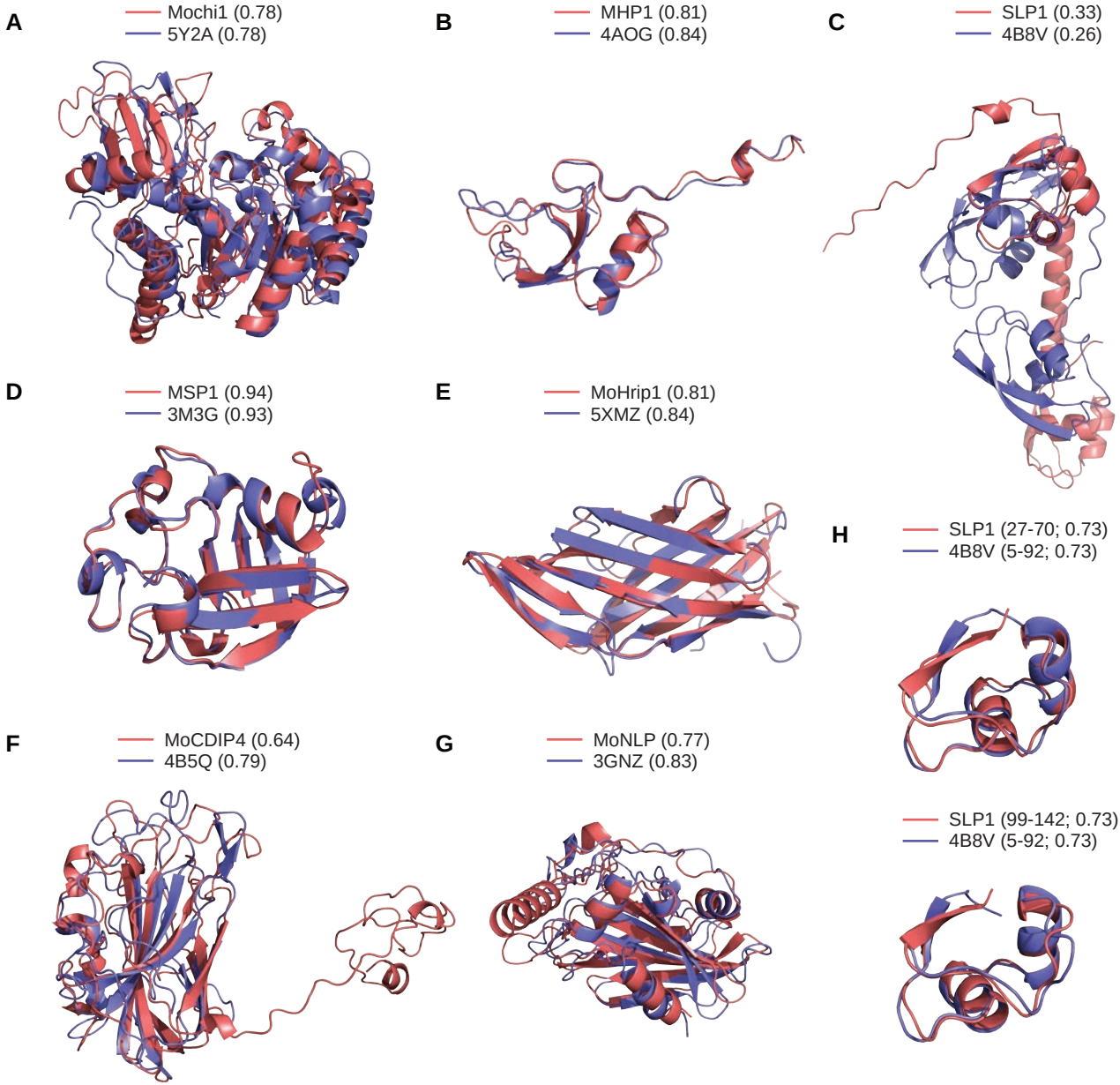

Figure S4. The structural superpositions of the predicted effectors against homologous structures identified with BLASTP

The predicted structure (red) was superposed against its homologous structure (blue) with TM-align. The TM-score normalized for each structure is indicated in the parentheses. **A,** MoChi1 and 5Y2A. **B,** MHP1 and 4AOG. **C,** SLP1 and 4B8V. **D,** MSP1 and 3M3G. **E,** MoHrip1 and 5XMZ. **F,** MoCDIP4 and 4B5Q. **G,** MoNLP and 3GNZ. **H,** SLP1 LysM domains (27-70; 99-142) and 4B8V LysM domain (5-92). Although predicted SLP1 structure was not similar to 4B8V, LysM domain was correctly modeled.

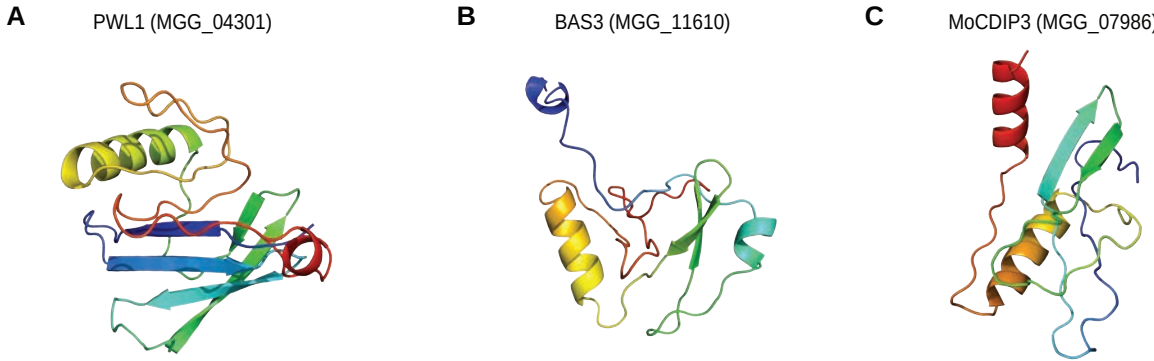

Figure S5. The structures of effectors with no homologous templates predicted with TrRosetta

A, PWL (MGG_04301; estimated precision of 0.56). **B,** BAS3 (MGG_11610; estimated precision of 0.53). **C,** MoCDIP3 (MGG_07986; estimated precision of 0.50).

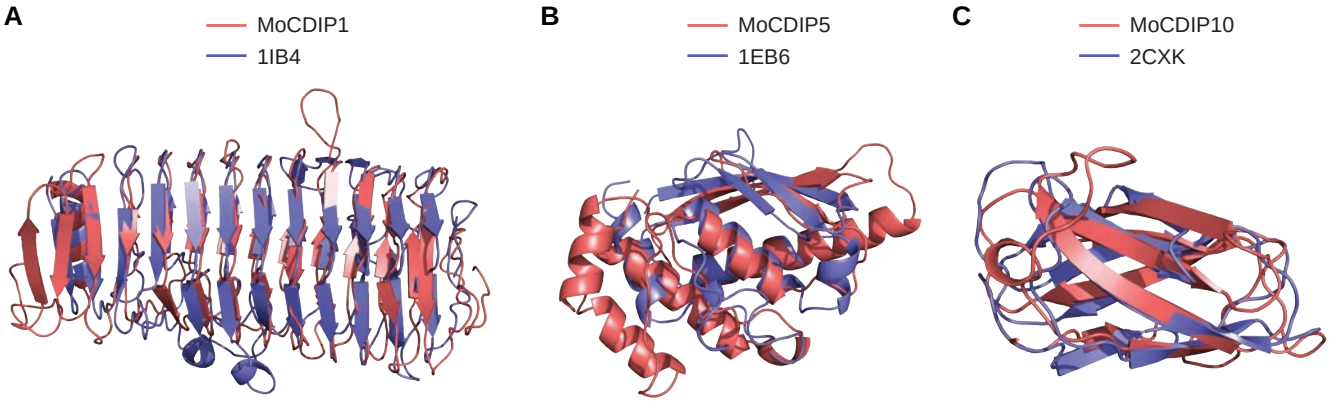

Figure S6. The structural superposition of MoCDIP1, 5 and 10 and their significant matches

The predicted structures (red) of MoCDIP1, 5 and 10 were superposed against their structural matches. The normalized TM-scores, as a measure of similarity, were **A,** 0.75 and 0.74 for MoCDIP1 and 1IB4, **B,** 0.52 and 0.61 for MoCDIP5 and 1EB6, and **C,** 0.64 and 0.63 for MoCDIP10 and 2CXK.

Figure S7. The structural similarity of the known MAX effectors

A pair of known MAX effectors was superposed to measure their structural similarity with TM-align. The TM-score was normalized for the structure given in each row. The TM-scores > 0.5 and ≤ 0.5 are indicated in red and blue.

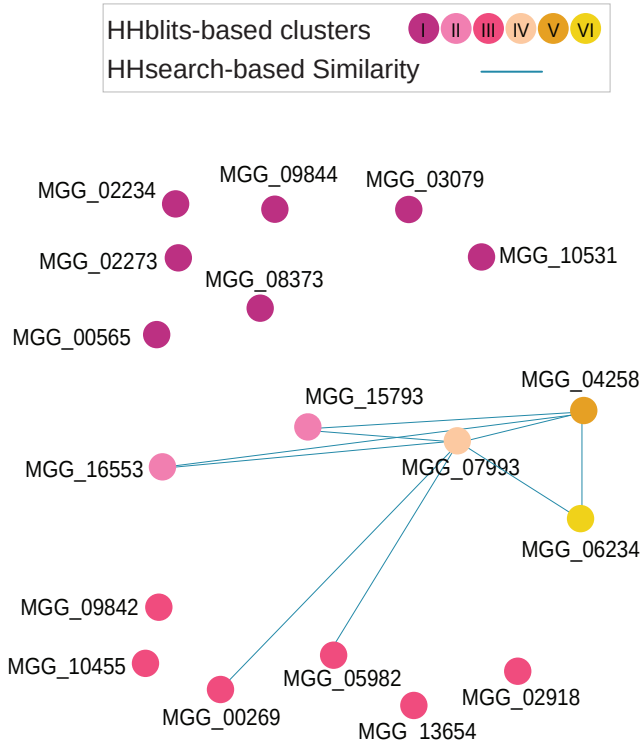

Figure S8. The network graph for Cluster 14

The memberships (HHblits-based clusters) are defined based on profile-to-sequence similarity search for Cluster 14 and indicated in different colors. Profile-to-profile similarity search was performed with HHsearch, and the edges indicate detectable homology by this method. The homology detected with HHsearch for the proteins in the same membership is not indicated.

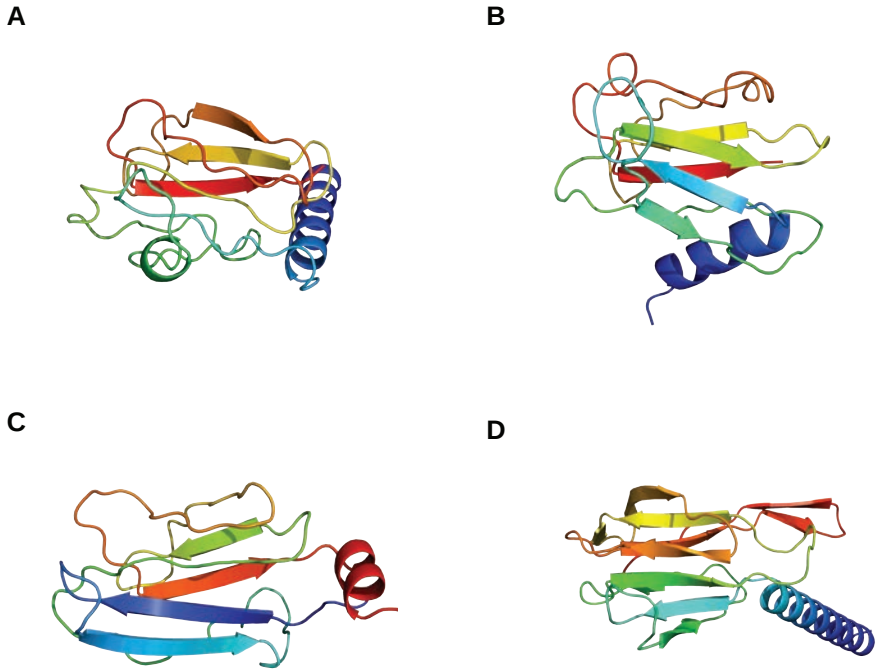

Figure S9. The structures of Ecp effectors from *Cladosporium fulvum* predicted by TrRosetta

A, Ecp4 (estimated precision of 0.56). **B,** Ecp7 (estimated precision of 0.68). **C,** Ecp29 (158-266; estimated precision of 0.60). **D,** Ecp30 (estimated precision of 0.66).

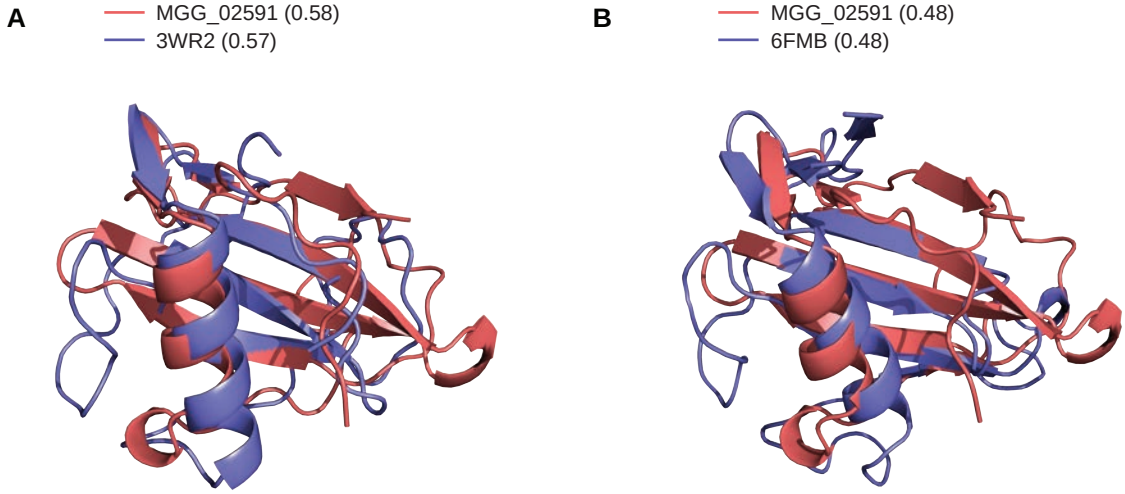

Figure S10. The structural superpositions between a predicted RNase and two RNase structures in the Protein Data Bank

The predicted structure of MGG_02591 (red) was superposed against the available RNase structures with TM-align. The normalized TM-score for each structure is indicated in the parentheses. **A,** RNase Po1 from *Pleurotus ostreatus* (3WR2). **B,** RNase-like effector from *Blumeria graminis* (6FMB).

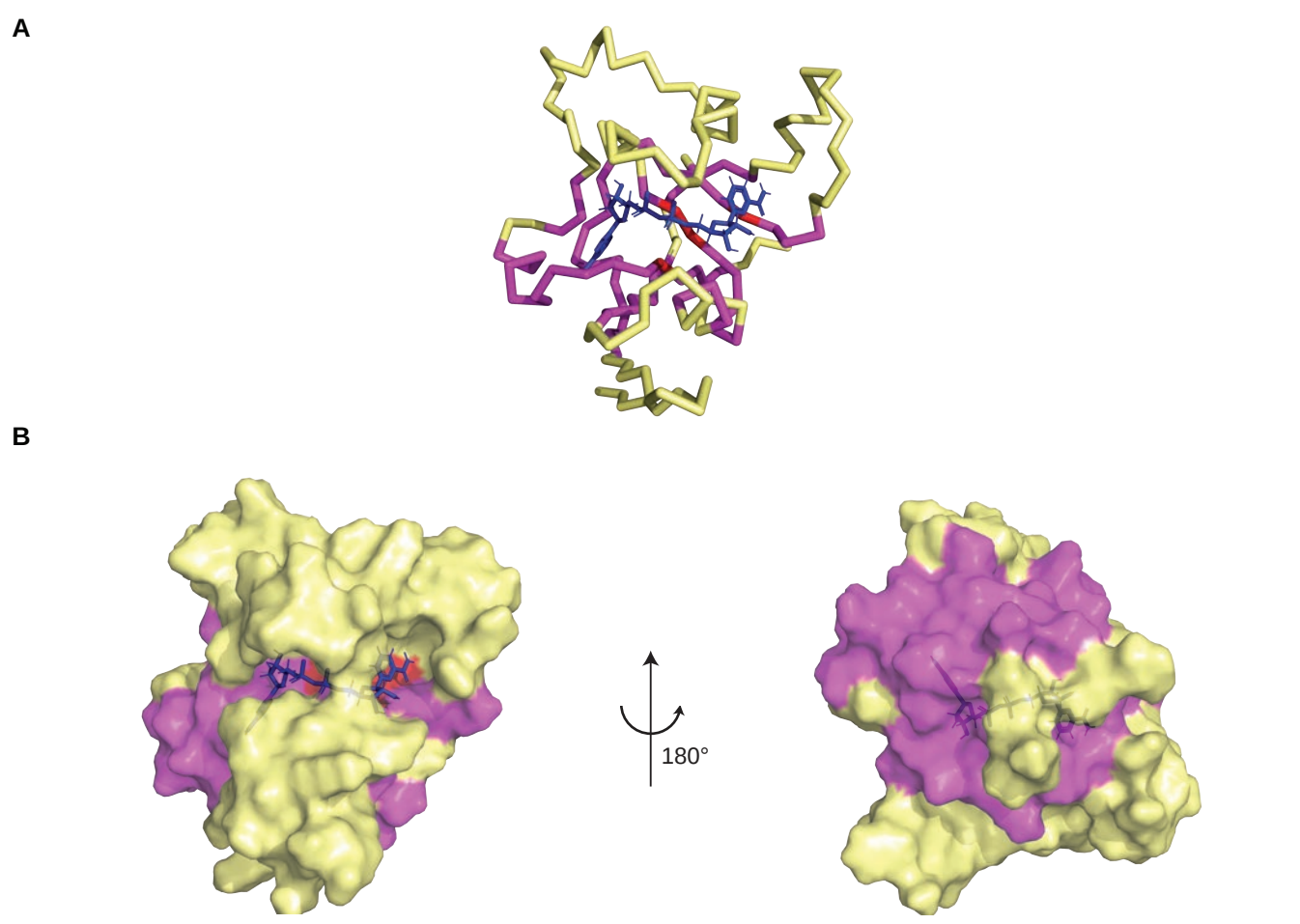

Figure S11. Docking NAD+ into a putative ADP-ribose transferase MGG_00230

An NAD+ molecule was docked into MGG_00230 by EDock. The conserved structural core shown in Figure 6C is indicated in magneta and the catalytic residues in red. **A,** A ribbon topology of MGG_00230. **B,** The surface structure of MGG_00230.

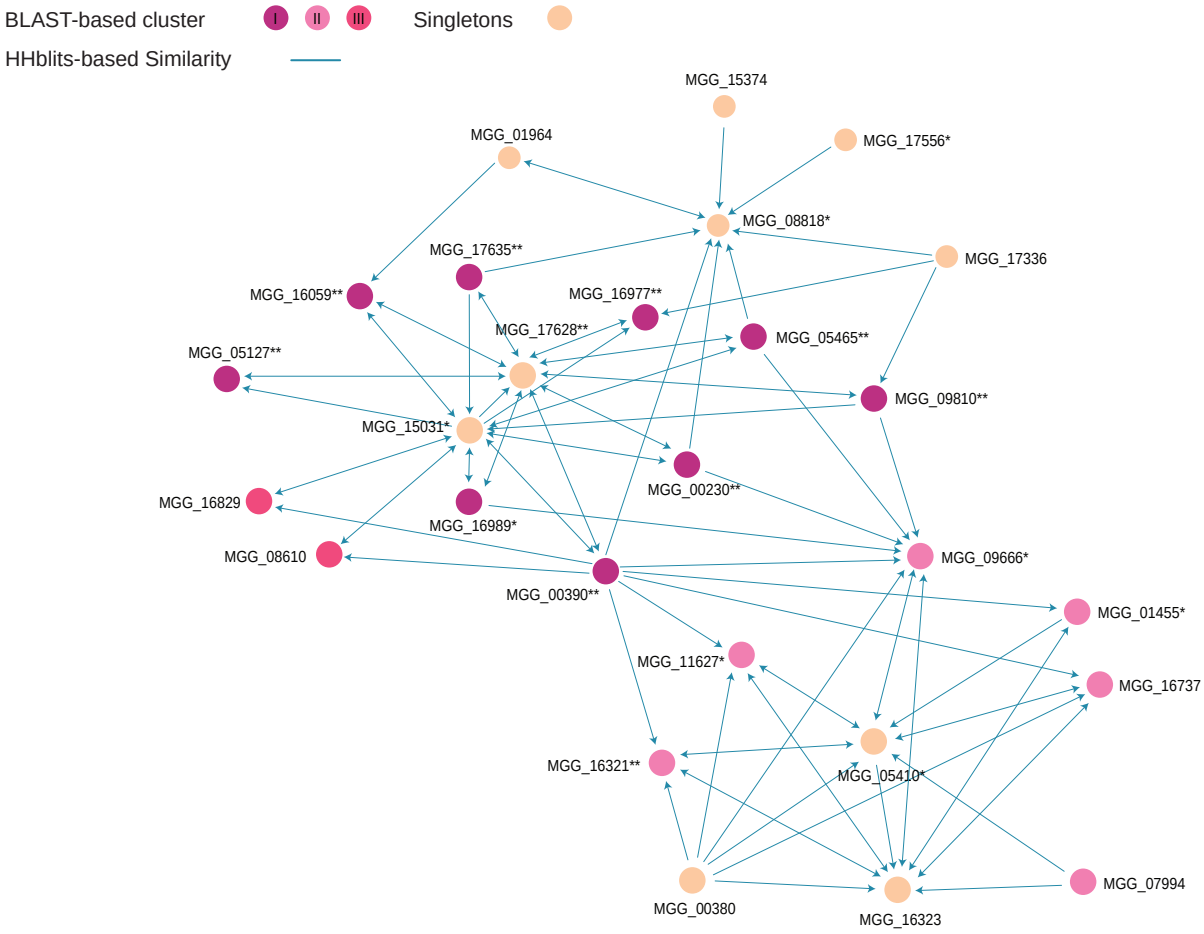

Figure S12. The homology-based network graph of Cluster 8

Each node indicates a member in Cluster 8. The BLAST-based membership is indicated by different colors of nodes. For instance, the 9 members in BLAST-based cluster II colored in purple are homologs detectable with BLAST. Profile-to-similarity search with HHblits was then performed to reveal additional homology between the proteins with different BLAST-based membership. This homology is indicated as edges. The arrow indicates the directionality of homology. For instance, MGG_00230 → MGG_09666 means HHblits with the profile of MGG00230 can identity homology to MGG_09666. * indicates that the protein has a predicted structure with expected precision > 0.5 for TrRosetta and > 0.55 for I-TASSER, and ** denotes that the predicted structure was classified to have the ADP-ribosylation fold, regardless of the confidence scores.

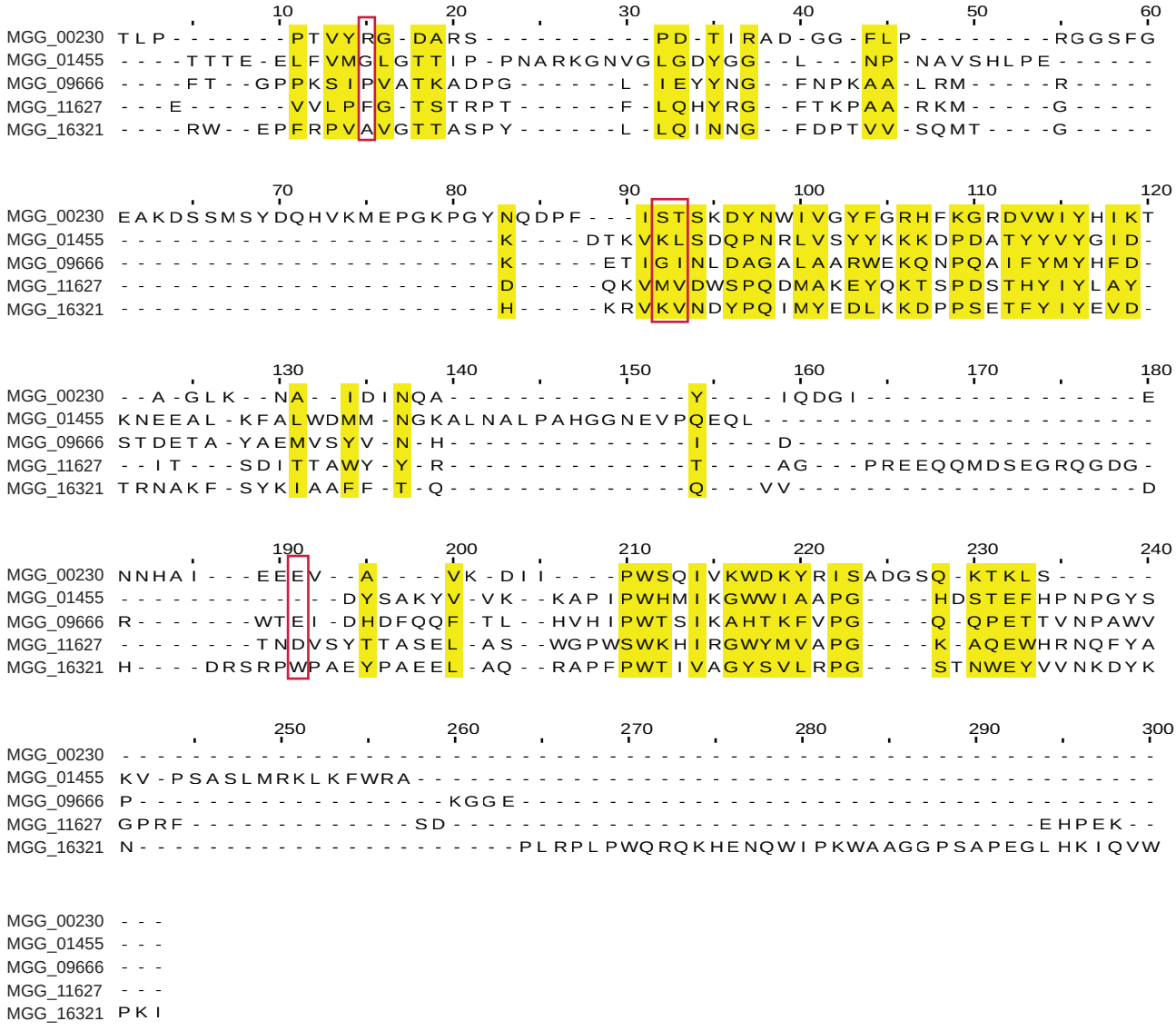

Figure S13. The structure-based alignment of secondary ARTs in the BLAST-based cluster II and a core ART, MGG_00230

The structures of the four secondary ARTs and a core ART, MGG_00230, were superposed with mTM-align, and the structural alignment was generated. The yellow highlight indicates columns with a conservation score > 3 annotated with Jalview. The red box indicates catalytic sites of MGG_00230.